SONAR-BASED ICEBERG-RELATIVE AUV LOCALIZATION

Peter Kimball[1]
pkimball@stanford.edu

Stephen Rock[1,2]
rock@stanford.edu

[1]Dept. of Aeronautics & Astronautics
Stanford University
496 Lomita Mall
Stanford, CA 94305

[2]Monterey Bay Aquarium Research Institute
7700 Sandholdt Road
Moss Landing, CA 95039

Abstract

This paper discusses the localization portion of a new iceberg-relative navigation technique for Autonomous Underwater Vehicles (AUVs). An estimator is presented which correlates incoming sonar range returns with an a-priori iceberg surface map in order to provide iceberg-relative AUV position and orientation estimates. The technique works by maintaining estimates not only of iceberg-relative AUV position and orientation, but also of the translational and rotational velocities of the iceberg itself. In addition to the a-priori iceberg surface map, required inputs to the estimator are measured inertial vehicle displacements and measured sonar range vectors from the vehicle to the iceberg.

Details of a particle filter implementation of the estimator are provided along with example localization results. The example data were collected from the RVIB *Nathaniel B Palmer* during circumnavigation of an iceberg in the Scoita Sea. In the example results, the vehicle position with respect to the berg is estimated to within 2 m, and the iceberg translational and rotational velocities are estimated to within 20%.

1 Introduction

Large free-floating icebergs are traveling ecosystems of great interest to science. Because they are relatively difficult and dangerous to approach, they are attractive targets for exploration by Autonomous Underwater Vehicles (AUVs). However, because they are moving and rotating, standard AUV navigation methods are unable to provide iceberg-relative position estimates. These estimates can be achieved by a new AUV navigation solution comprised of two steps: mapping and localization. The mapping step was described in a recent paper [1]. The localization step is presented here.

Figure 1: Photograph of iceberg used for experiment

To operate in the under-ice environment, an AUV must possess some capability of navigation with respect to the ice surface. Existing under-ice AUV navigation systems have typically relied on dead-reckoning using inertial measurements and/or velocity measurements from a Doppler sonar (both seafloor-relative and ice-relative). These systems have been used successfully to move between pre-programmed waypoints in horizontal inertial space, with depth determined by reactive terrain-following (or ice-following) and obstacle avoidance behaviors. However, these existing systems cannot provide accurate ice-relative position estimates around free-floating, rotating icebergs. Specifically, accelerom-

eters, gyros, and compasses provide information about how the AUV moves with respect to an inertial frame, not with respect to the ice. And while Doppler Velocity Loggers (DVLs) can provide ice-relative velocity measurements, they cannot account for any rotation of the ice. Hence, extensions to the navigation system are required to enable AUV navigation around free-floating icebergs.

Using the localization technique presented in this paper, an AUV revisiting a previously-mapped iceberg can know its position in the map, enabling safe operation near the iceberg, and the capability to return to sites of interest. The localization technique is terrain-relative, using correlation between incoming sonar measurements and the a-priori iceberg terrain map to provide an iceberg-relative vehicle position estimate. The technique works by maintaining estimates not only of iceberg-relative vehicle position and orientation, but also of the translational and rotational velocities of the iceberg itself. This paper presents details of the algorithm along with example localization results performed using a set of ship-based multibeam sonar data taken from an Antarctic iceberg (pictured in Figure 1). In this example, the vehicle position with respect to the berg is estimated to within 2 m, and the iceberg translational and rotational velocities are estimated to within 20%.

2 Background

2.1 AUV Navigation Beneath Sea Ice

The inherent difficulty of accessing the under-ice environment has driven an increase in the capability of AUVs to operate at high latitudes and under sea ice [2]. AUV navigation in this environment is made challenging by the inability of AUVs to obtain GPS navigation fixes while beneath ice, by the reduced performance of navigation instruments at high-latitudes [3], and by the hazardous presence of both ice and seafloor obstacles. Nevertheless, many successful AUV missions have been performed beneath sea ice. These missions have all utilized some form of dead-reckoning navigation, with a variety of drift-correction techniques.

In its Arctic configuration, MIT Sea Grant's Odyssey II vehicle used only angular rate and acceleration sensors to derive vehicle attitude and heading. Drift in this estimate was corrected by magnetic field intensity measurements in all three vehicle axes, however this was done post-mission and was not an aid to navigation. Position estimation for vehicle navigation was achieved through the use of pre-deployed long baseline (LBL) or ultra-short baseline (USBL) acoustic systems. In addition, Odyssey II used an acoustic homing beacon as a directional reference when returning to a recovery location. During successful deployment in the Beaufort Sea (Arctic), an upward-looking sonar on Odyssey II created a record of ice-draft above the vehicle's navigation track [4].

The Canadian AUV, Theseus, was designed to lay several kilometers of fiber-optic cable beneath Arctic ice. Theseus navigated to predetermined position waypoints using dead-reckoning, based on acceleration measurements from an IMU and velocity measurements from bottom-pinging Doppler sonar. The dead-reckoned position estimate drifted at a rate of 0.5% of distance traveled (%DT). To achieve an order of magnitude improvement in navigation (to 0.05%DT), the dead-reckoned estimate was updated with position fixes from multiple acoustic beacons, installed at pre-surveyed locations along the desired vehicle path [5].

In October 2001, the Monterey Bay Aquarium Research Institute operated the ALTEX AUV in the Arctic to test the operation of various navigation instruments at high latitudes. Dead-reckoning using bottom-pinging (or ice-pinging) Doppler sonar, the ALTEX vehicle achieved position error better than 0.05%DT, without the use of external navigation aids (such as an LBL array). Under-ice missions on this deployment were approximately 5km long [3].

In February 2002, a Cambridge team deployed a Martin 150 AUV in East Greenland pack ice to obtain the first AUV-based sidescan sonar imagery of arctic pack ice. The Martin Positioning (MARPOS) system relied on dead-reckoning integration of inertial accelerations, angular rates from a ring-laser gyro, and velocities from bottom-pinging Doppler sonar. This system achieved 0.1%DT horizontal error, as long as bottom-pinging was possible. The vehicle used differential GPS at the surface to obtain periodic position fixes [6]. In April 2007, another Cambridge team used an ice-lanuched Gavia vehicle to obtain three-dimensional digital terrain maps of the underside of sea ice in the Beaufort Sea. This vehicle maintained a position estimate by dead-reckoning with ice-pinging Doppler sonar, and was recovered via a tether [7].

The British Autosub Under Ice (AUI) program has deployed the Autosub AUV under both Arctic and Antarctic sea ice. AUI missions in Greenland [8] and Antarctica [9] returned three-dimensional images of under-ice topography, taken with upward-looking swath sonar from the AUV. Autosub utilized reactive obstacle avoidance for these missions,

but was navigated using dead-reckoning techniques in which velocity measurements were made using bottom-pinging or ice-pinging Doppler sonar. Autosub navigated to its recovery point by following a ship-deployed acoustic homing beacon.

2.2 Terrain-Relative Navigation

TRN systems are used to eliminate accumulated drift error in vehicle position estimates by correlating terrain contour measurements with a-priori terrain maps. The Terrain Contour Matching (TERCOM) algorithm was one of the first implementations of this principle, and was used to correct drift in cruise missile navigation systems for many years [10]. Sequences of single-beam altitude measurements from along missile trajectories form the inputs to the TERCOM algorithm.

More recently, TRN techniques have been used (in place of GPS or acoustic transponder arrays) to correct drift error in underwater vehicle systems. Implementations have been fielded which provide real-time corrections to vehicle navigation, while others are used in post-processing [11–13]. In all implementations, the achievable precision and accuracy of the navigation estimates are limited by the resolution and quality of the a-priori map. Furthermore, the terrain in the operating area must have sufficient texture to be used in identifying vehicle position - TRN techniques provide no benefit over large areas of completely flat terrain.

2.3 Bayesian Estimators

In many applications (including underwater TRN), vehicle position estimates are often multimodal probability distributions, which are not well approximated by unimodal Gaussians or other parameterized distributions. A number of Bayesian techniques have been developed for estimation problems with nonlinear belief distributions. The goal of any Bayesian estimator is to approximate the posterior probability distribution, $p(x_k|z_{1:k}, u_{1:k})$. In vehicle localization, this is the probability that a given vehicle state, x_k, represents the truth at epoch, k, conditioned upon all previous sensor measurements, $z_{1:k}$, and all previous vehicle controls, $u_{1:k}$.

Particle filters and point mass filters are examples of Bayesian estimators. [14] shows that each of these is suitable for underwater TRN, and that the localization accuracy of either method is approximately equal to the horizontal resolution of the terrain map used. [14] also concludes that the point mass filter is slightly more accurate and robust than the particle filter, but that its computational expense increases dramatically with additional state dimensions. This work uses a particle filter due to the additional states used to estimate terrain motion.

2.4 Particle Filters

Particle filters represent the posterior, $p(x_k|z_{1:k}, u_{1:k})$, with a set of random state samples drawn from the posterior. Ideally, the probability of a particular state, x_k, being included in the set of samples is proportional to its Bayes posterior [15]. To achieve this, particle filters rely on incorporation of vehicle sensor measurements into a periodic resampling of the particle distribution. After every measurement, each particle is assigned a weight equal to the probability of making that measurement, z_k given that particle's state, x_k. These weights are often expressed as exponentials, allowing them to be updated multiplicatively following each new measurement. When appropriate, a resampling step then throws out particles with low weights, and replaces them with new particles in highly-weighted regions of the state space. In this way, the particle filter uses a finite number of particles efficiently - only in likely regions of the state space.

3 Problem and Approach

For TRN, map-correlation of a single (2-dimensional) multibeam sonar ping is generally insufficient to uniquely identify the position of the vehicle. Rather, several pings (giving a 3-dimensional representation of the surface) are required to localize a vehicle. The central problem in using TRN around a free-floating iceberg is that in order to use multiple pings, the ice-relative displacement of the vehicle between pings must be known, yet only the inertial displacement of the vehicle is readily measured.

Typical iceberg motion (although varied geographically) involves 0.03–0.08 m/s translational speeds, and 5–10 deg/hr rotation rates, while translational speeds up to 0.27 m/s and rotation rates up to 40 deg/hr have been observed [16], [17]. Given an AUV operating speed of 1.75 m/s, this typical iceberg motion represents a drift rate of 1.7 to 4.6 percent of distance traveled (%DT). Compared with the 1%DT error achieved by high-accuracy dead-reckoning positoning systems, this motion is significant.

However, while iceberg velocities are significant, they also change very slowly compared to the up-

date rate of a TRN estimator. Hence, they can be estimated explicitly as slowly-changing parameters, and accounted for during each motion update. This way, after several motion updates, measurement updates will allow the estimator to learn not only the berg-relative vehicle position, but also the inertial velocities of the berg.

Specifically, the estimator presented here estimates the following nine degrees of freedom: all three iceberg-relative vehicle position states, all three iceberg-relative vehicle orientation states, an Easterly iceberg velocity, a Northerly iceberg velocity, and an iceberg heading rate. It requires inertial measurements of vehicle position and orientation (for motion updates), as well as multibeam sonar measurements of range to the iceberg surface (for map-correlation in measurement updates).

AUVs are commonly equipped with Doppler velocity loggers (DVLs) which can provide ice-relative vehicle velocity information. Lacking an iceberg-relative heading reference, this sensor does not completely solve the iceberg-relative navigation problem, but does provide a measurement which will be useful in future versions of the localization algorithm. Because no DVL instrument was available during collection of the data presented here, the algorithm detailed below does not utilize Doppler velocity measurements.

4 Algorithm

While various Bayesian estimator TRN formulations could appropriately be extended to estimate iceberg velocities, this work utilizes the particle filter formulation due to the ease and efficiency with which particle filters handle the estimation of larger numbers of state variables. Each particle represents a hypothesized system state, and is defined completely by its weight and the values of its nine states - position and orientation with respect to the iceberg and iceberg northerly, easterly, and heading rates. Together, all the particle weights form a sample-based approximation to the posterior probability density distribution, $p(x_k|z_{1:k}, u_{1:k})$, where each z is a multibeam sonar measurement, and each u is a measured vehicle displacement.

The particle filter algorithm consists of three steps, and is run every time a new multibeam sonar measurement is recorded (each epoch, k). First, the particles undergo an iceberg-relative motion update. Second, the particle weights undergo a measurement update based on map-correlation of the new multibeam measurement. Third, the particle distribution may be resampled in order to allocate particles to the most meaningful regions of the state space.

The motion update step of the particle filter algorithm adds the ice-relative vehicle displacement (since the last update) to each particle. This relative displacement is calculated as the difference between the measured inertial vehicle displacement and the estimated inertial iceberg displacement. The displacement added to each particle also includes an additive Gaussian random noise term, sized to represent the uncertainty in the measured inertial vehicle displacement. The contribution to the motion update due to inertial iceberg displacement is different for each particle since each particle maintains its own iceberg velocity estimates. For each motion update, these velocities are treated as constant over the period of the update. However, small Gaussian random noise is added to each particle's iceberg velocity estimates between motion updates such that slow changes in the iceberg motion can be learned.

Equation (1) details the motion update step for the m^{th} particle between epochs $k-1$ and k. Each particle's state vector represents a hypothesis over iceberg-relative vehicle position (x, y, and z) and orientation (ϕ, θ, and ψ), as well as the Northerly, Easterly, and heading rates of the iceberg through inertial space ($\dot{X}_{\text{ice}}$, $\dot{Y}_{\text{ice}}$, and $\dot{\Psi}_{\text{ice}}$). The measured displacements in the six vehicle pose states (Δx through $\Delta\psi$) come from an inertial measurement unit. ν is a zero-mean, unit-variance normally distributed random noise vector, sized by $\mathbf{\Sigma}_{\text{IMU}}^{6\text{x}6}$ (usually diagonal) to account for uncertainty in the inertial displacement measurements, and by $\mathbf{\Sigma}_{\text{ice}}^{3\text{x}3}$ (usually diagonal) to allow for slow changes in iceberg motion parameters. $\mathbf{R}_k^{[m]}$ is the 2x2 rotation matrix which transforms vectors from the inertial frame to the iceberg frame. This rotation is based on the the iceberg's heading, which is not explicitly estimated as a state, but rather computed for the m^{th} particle as the difference between the vehicle (inertial) compass heading and $\psi_k^{[m]}$, the particle's estimate of the iceberg-relative vehicle heading.

The measurement update step computes and normalizes the weights of the particles. For each particle, the weight is proportional to the probability of making all multibeam measurments since the last resampling operation, given the trajectory of that particle. This update is recursively computed after each measurement by multiplicatively updating each particle weight based on the likelihood of making only the current measurement given the particle's current position. For the m^{th} particle, each update term takes the form given in Equation (2), where $\mathbf{z}_k$ is a the current measurement vector, and

$$\begin{bmatrix} x \\ y \\ z \\ \phi \\ \theta \\ \psi \\ \dot{X}_{\text{ice}} \\ \dot{Y}_{\text{ice}} \\ \dot{\Psi}_{\text{ice}} \end{bmatrix}_k^{[m]} = \begin{bmatrix} x \\ y \\ z \\ \phi \\ \theta \\ \psi \\ \dot{X}_{\text{ice}} \\ \dot{Y}_{\text{ice}} \\ \dot{\Psi}_{\text{ice}} \end{bmatrix}_{k-1}^{[m]} + \begin{bmatrix} \Delta x \\ \Delta y \\ \Delta z \\ \Delta \phi \\ \Delta \theta \\ \Delta \psi \\ 0 \\ 0 \\ 0 \end{bmatrix} - (t_k - t_{k-1}) \begin{bmatrix} \mathbf{R}_k^{[m]} & \mathbf{0} \\ \mathbf{0} & \mathbf{0} \end{bmatrix} \begin{bmatrix} \dot{X}_{\text{ice}} \\ \dot{Y}_{\text{ice}} \\ 0 \\ 0 \\ 0 \\ \dot{\Psi}_{\text{ice}} \\ 0 \\ 0 \\ 0 \end{bmatrix}_{k-1}^{[m]} + \begin{bmatrix} \mathbf{\Sigma}_{\text{IMU}}^{6\text{x}6} & \mathbf{0} \\ \mathbf{0} & \mathbf{\Sigma}_{\text{ice}}^{3\text{x}3} \end{bmatrix} \nu \tag{1}$$

$$w_k^{[m]} = p(z_k | x_k^{[m]}) = \frac{1}{\sqrt{2\pi |\mathbf{\Sigma}|}} \exp \left[-\frac{1}{2} (\mathbf{z}_k^{[m]} - \mathbf{a}_k^{[m]})^{\mathrm{T}} \mathbf{\Sigma}^{-1} (\mathbf{z}_k^{[m]} - \mathbf{a}_k^{[m]}) \right] \tag{2}$$

$\mathbf{z}_k^{[m]}$ is the projection of the measurement into the map frame under the particle's state, $\mathbf{x}_k^{[m]}$, and $\mathbf{a}_k^{[m]}$ is the vector of points on the iceberg surface which are closest to their corresponding measurement points in $\mathbf{z}_k^{[m]}$. Thus, the vector $\mathbf{z}_k^{[m]} - \mathbf{a}_k^{[m]}$ is the measurement error vector, representing the distance from the mapped iceberg face of each projected sounding in the current measurement.

In this common Gaussian model for measurement error, the particle weight is assigned according to the assumption that the probability of a set of measurement errors is a zero-mean Gaussian, with covariance given by $\mathbf{\Sigma}$. Here, $|\mathbf{\Sigma}|$ becomes σ^{2n} (where n is the number of beams being used in the measurement) under the assumptions that the beam measurement errors are uncorrelated and that the measurement variance, σ^2, is the same for each beam.

Resampling is only performed when two conditions have been met. First, a sufficiently high number of soundings must have been used to calculate the particle weights. Second, the variance of the particle weights must be sufficiently high. These two requirements prevent particle deprivation - a loss of diversity in the particle distribution. When sampling is performed, it is done according to the low-variance sampling algorithm presented in [15], which avoids particle deprivation and is inexpensive to perform. A small, normally distributed noise term is added to each state of a resampled particle in order to explore the nearby state space.

5 Experimental Results

5.1 The Data Set

In June 2008, multibeam sonar data were taken from an iceberg in the Scotia Sea. During data collection, the berg translated at approximately 0.09 m/s (0.18 kts), and rotated at approximately 20 deg/hr. The sonar data were recorded by a sideways-looking 400KHz Reson multibeam sonar head mounted on a pole 10 m beneath the RVIB *Nathaniel B Palmer* (see Figure 2).

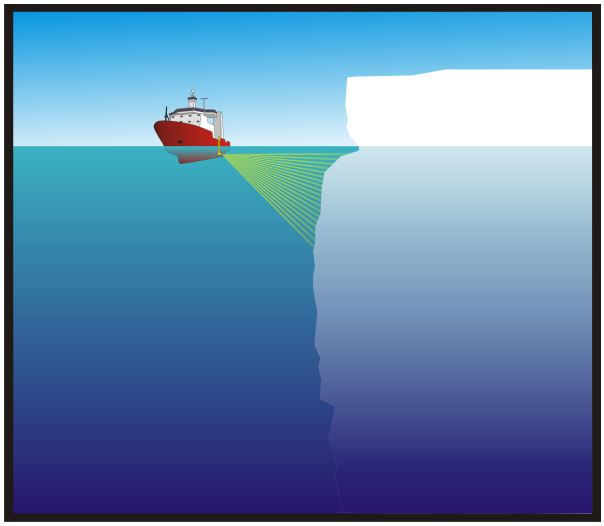

Figure 2: Sideways-looking multibeam sonar beneath the R.V. Nathaniel B Palmer

The ship's track in inertial space was measured by GPS. Sonar imagery of the shallowest 250 m (approximately) of the iceberg's submerged perimeter was collected as the ship made a steady 400 ° circumnavigation of the berg in just under 40 minutes. A photograph of the iceberg appears in Figure 1.

5.2 Data Processing

Each multibeam sonar ping is tagged with the orientation and GPS position of the ship at the time of the ping. Raw sonar data were edited using the open-source, NSF-supported MB-System software

package. Bad beams (e.g. max range, zero range, or excessive noise) were flagged using MB-System. The differential location between the ship's position sensors and the multibeam sensor was added to the vehicle-frame sonar range vectors.

5.3 The A-Priori Map

The multibeam sonar soundings were assembled into a self-consistent map, representing the shape of the iceberg (as described in [1]). This map appears in Figure 3. Since the publication of [1], the map has been updated to include further cleaning of the sonar data and a refined approximation of error smoothing (corresponding with an assumed constant iceberg motion) used for the mapping. Note that there are sections of the iceberg where sufficient map data could not be collected, and the map surface is left undefined. As the vehicle passes by these regions of the berg, measurement updates (map correlations) for localization are not possible.

In order to speed the terrain correlation computation, and allow for surface plotting of the iceberg map, the map data have been reduced by the following method. All soundings were transformed into a cylindrical coordinate system (azimuth, depth, range) centered over the iceberg. The range data were then gridded over azimuth and depth. In each cell with five or more soundings, the average range value forms a surface point estimate along with the azimuth and depth values for that cell. Grid cells with fewer than five soundings are not assigned a surface point. The Delaunay triangulation over all surface points defines the triangular surface patches used for plotting. Superior (more probabilistically appropriate) methods for surface recovery and decimation representation exist in the computer graphics literature, and must be implemented in mapping icebergs whose surfaces cannot be well approximated by cylinders.

In this experiment, the same multibeam sonar data are being used to localize the vehicle within the map as were used to create the map in the first place. This means that the assumed iceberg motion used to create the map can be considered truth, since the map projection depends entirely on that motion. Thus, if the estimator were to perform perfectly, it would yield an iceberg motion estimate exactly matching the assumed motion. Ideally, there would also exist a second sonar data set, along with GPS ground-truth for the iceberg motion so that the envisioned operational case of localization during a re-visit to a previously-mapped iceberg could be tested. Unfortunately, such a data set was not collected.

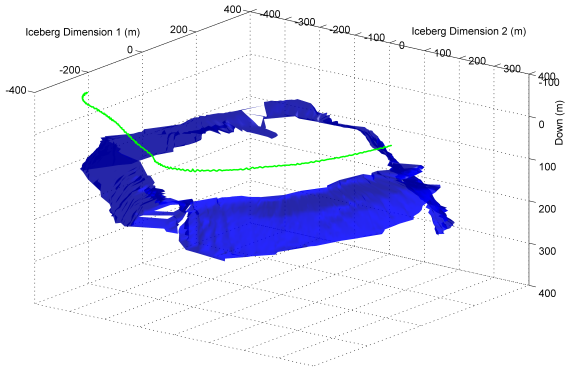

Figure 3: Iceberg Map and Segment of Vehicle Trajectory

5.4 Localization Results

In this experiment, the estimator is initialized to a broad distribution, and converges to a useful estimate of system state after a series of motion and measurement updates. Approximately four seconds pass between measurement updates. Figures 4 and 5 show the vehicle pose and iceberg velocity estimation errors, respectively. Each of the smaller, magenta dots represents a hypothesized state value corresponding to a single particle. The larger, blue dots represent the weighted mean of the distribution. (Since depth, roll, and pitch are readily measured, estimation errors for these parameters are not shown).

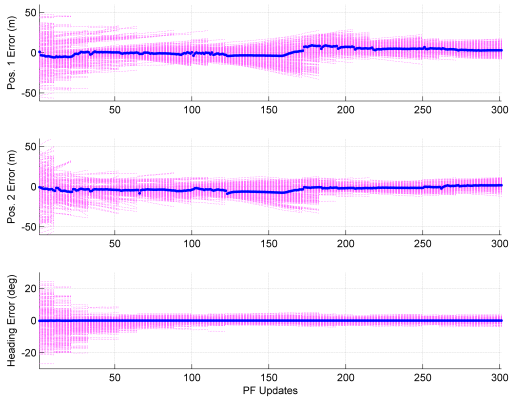

Figure 4: Iceberg-relative vehicle pose estimation errors

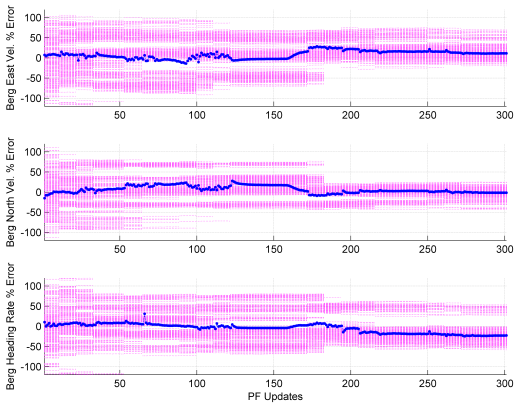

Figure 5: Iceberg velocity estimation errors

Following convergence, the error in the weighted mean of the distribution is less than 2 m for the iceberg-relative position states, less than 1 degree for the iceberg-relative vehicle heading, less than 10% for the iceberg translational velocity estimates, and less than 20% for the iceberg heading rate estimate. Note that very few map correlations (measurement updates) are possible due to holes in the map between updates 125-170. Thus, the distribution isn't resampled during this period, and it spreads out. However, when measurement updates become available again, the distribution can be resampled, and converges once again. The ability of the motion updates to keep the position estimates reasonable in the absence of measurement updates depends on how well the iceberg motion state estimates have converged before the measurement updates become impossible.

5.5 Initialization

The more closely an estimator can be initialized to the true distribution, the less time it will take to converge. However, the initial distribution must be set realistically based on the capability of AUV operators to estimate the system state at the time of an AUV's deployment. While this capability varies based on experience and available instrumentation, the independent Gaussian parameter distributions used for initialization in the present example are listed in Table 1. These distributions can also be seen visually in Figures 4 and 5 as the magenta points in the first column.

Table 1: Initial Distribution

Parameter	**Units**	**Mean**	**Var**
Relative Vehicle Pos. 1	m	27.84	20
Relative Vehicle Pos. 2	m	292.30	20
Vehicle Depth	m	0.13	0.1
Vehicle Roll	deg	1.14	0.1
Vehicle Pitch	deg	5.34	0.1
Relative Vehicle Heading	deg	179.47	10
Iceberg North Velocity	m/s	-0.05	0.02
Iceberg East Velocity	m/s	0.08	0.04
Iceberg Heading Rate	deg/hr	20.63	6.55

5.6 Tradeoffs

As with any estimator implementation there are tradeoffs to be considered in implementing this particle filter. Map correlation of each sounding for each particle is the most expensive step in the algorithm. Three parameters which strongly influence the computation time are the number of particles (300 were used here), the measurement update period (4 seconds was used here, approximately 10 times slower than the maximum update rate of the sonar), and the number of beams from each multibeam ping which are actually used for correlation (492 were used here). The estimation performance tradeoff between precision and robustness is affected by the minimum number of soundings (individual beam measurements) required before resampling (5000 was used here), and the size of the exploratory noise added to particle states during resampling. Choices in these trades depend strongly on the uncertainty characteristics of the available sensors.

6 Conclusion

Typical iceberg motion is significant enough that existing AUV navigation methods are insufficient for navigation with respect to free-floating icebergs. A terrain-relative navigation (TRN) estimator has been presented which performs measurement updates using correlation between incoming multibeam sonar ranges and an a-priori iceberg surface map. A key feature of this technique is the explicit estimation and incorporation into the motion update of iceberg translational and heading velocities. Once the estimator has converged to a correct estimate of terrain motion, it is robust to areas of textureless terrain and to periods of time when multibeam measurements may be unavailable. Successful implementation of the estimator was demonstrated

using ship-based sonar data taken from an iceberg in the Scotia Sea.

During initialization (and assuming sufficiently textured terrain), the estimates of position states converge quickly because the measurement update depends directly on position. However, several motion updates must occur before errors in iceberg motion state estimates are manifested as position errors and therefore penalized during during the measurement update. Estimates of the iceberg velocities therefore require more time to converge. A further extension to the estimator would allow separate resampling of the vehicle position and iceberg motion states based on whether the position estimate had converged.

In this experiment, a very rough grid-based technique was used to reduce the map data to a surface representation. A better surface representation of the map would improve the performance of the algorithm, and will be required in order for the algorithm to be used with icebergs whose shapes are not well approximated by cylinders. Automation of the sonar data cleaning process will also be required for a truly autonomous, deployable version of the algorithm.

Acknowledgment

This work was supported by grant ANT-0811399 from the National Science Foundation. The authors would like to thank Reson Inc for the use of their 7125 sonar system, Brett Hobson for deploying and operating the sonar system, Joanna O'Neill for collecting and processing the multibeam data, and Dave Caress for his expertise and help with MBSystem.

References

[1] Peter Kimball and Stephen Rock, "Sonar-Based Iceberg-Relative AUV Navigation", in *Proceedings Of AUV2008*, Woods Hole, MA, October 2008, IEEE.

[2] Nicole Tervalon and Richard Henthorn, "Ice profiling sonar for an auv: Experience in the arctic", in *OCEANS*. MTS/IEEE, October 2002, vol. 1, pp. 305–310.

[3] Rob McEwen, Hans Thomas, Don Weber, and Frank Psota, "Performance of an auv navigation system at arctic latitudes", *IEEE Journal of Oceanic Engineering*, vol. 30, no. 2, pp. 443–454, April 2005.

[4] J.G. Bellingham, C.A. Goudey, T.R. Consi, J.W. Bales, D.K. Atwood, J.J. Leonard, and C. Chryssostomidis, "A second generation survey auv", in *Symposium on Autonomous Underwater Vehicle Technology*. AUV Technology, July 1994, pp. 148–155.

[5] Bruce Butler and Ron Verrall, "A precision hybrid inertial/acoustic navigation system for a long-range autonomous underwater vehicle", in *AM 98*. Institute of Navigation, 1998, pp. 561–572.

[6] P. Wadhams, J. P. Wilkinson, and A. Kaletzky, "Sidescan sonar imagery of the winter marginal ice zone obtained from an auv", *AMS Journal of Atmospheric and Oceanic Technology*, vol. 21, pp. 1462–1470, 2004.

[7] P. Wadhams and MJ Doble, "Digital terrain mapping of the underside of sea ice from a small AUV", *Geophysical Research Letters*, vol. 35, no. 1, 2008.

[8] P. Wadhams, J.P. Wilkinson, and S.D. McPhail, "A new view of the underside of arctic sea ice", *Geophysical Research Letters*, vol. 33, February 2006.

[9] K. W. Nicholls, E. P. Abrahamsen, J. J. H. Buck, P. A. Dodd, C. Goldblatt, G. Griffiths, K. J. Heywood, N. E. Hughes, A. Kaletzky, G. F. Lane-Serff, S. D. McPhail, N. W. Millard, K. I. C. Oliver, J. Perrett, M. R. Price, C. J. Pudsey, K. Saw, K. Stansfield, M. J. Stott, P. Wadhams, A. T. Webb, and J. P. Wilkinson, "Measurements beneath an antarctic ice shelf using an autonomous underwater vehicle", *Geophysical Research Letters*, vol. 33, April 2006.

[10] J. P. Golden, "Terrain contour matching (tercom) - a cruise missile guidance aid", in *Image Processing for Missile Guidance*. SPIE, July 1980, vol. 238, pp. 10–18.

[11] Ingemar Nygren and Magnus Jansson, "Terrain navigation for underwater vehicles using the correlator method", *IEEE Journal of Oceanic Engineering*, vol. 29, no. 3, pp. 906–915, July 2004.

[12] Ryan Eustice, Richard Camilli, and Hanumant Singh, "Towards bathymetry-optimized doppler re-navigation for auvs", in *OCEANS*. MTS/IEEE, 2005, vol. 2, pp. 1430–1436.

[13] S. Williams and I. Mahon, "A terrain-aided tracking algorithm for marine systems", *The International Conf on Field and Service Robotics*, pp. 112–118, 2003.

[14] Kjetil Bergh Ånonsen and Oddvar Hallingstad, "Terrain aided underwater navigation using point mass and particle filters", in *Position, Location, And Navigation Symposium, 2006.* IEEE/ION, April 2006, pp. 1027– 1035.

[15] S. Thrun, W. Burgard, and D. Fox, *Probabilistic Robotics (Intelligent Robotics and Autonomous Agents)*, MIT press, Cambridge, Massachusetts, USA, 2005.

[16] R. Gladstone and G.R. Bigg, "Satellite tracking of icebergs in the weddell sea", *Antarctic Science*, vol. 14, no. 03, pp. 278–287, 2002.

[17] P. Wadhams and M. Kristensen, "The response of antarctic icebergs to ocean waves", *Journal of geophysical research*, vol. 88, no. C10, pp. 6053–6065, 1983.